AJBS Asian Journal of Biological Sciences

OPEN ACCESS

Integrated *in vitro* and *in silico* Approaches for the Management of Sunflower Anthracnose Caused by *Lasiodiplodia pseudotheobromae*

[1,2]*Maniruzzaman Sikder*, [1]*Sabbir Ahmmed*, [1]*Nazmussakib Shuvo*, [1]*Sayma Sajuti*, [1]*Farhana Rahman and* [1]*Nuhu Alam*

[1]*Department of Botany, Jahangirnagar University, Dhaka 1342, Bangladesh*

[2]*Department of Plant, Food and Environmental Sciences, Dalhousie University, Nova Scotia, Canada*

Corresponding Author: Maniruzzaman Sikder (mmsbot@juniv.edu)

ABSTRACT

Background and Objective: Sunflower production is severely constrained by anthracnose disease caused by *Lasiodiplodia pseudotheobromae*, highlighting the need for effective and environmentally sustainable disease management strategies. This study aimed to evaluate the effects of different culture media and temperatures on fungal vegetative growth, determine the antifungal efficacy of biological control agents, plant extracts, and chemical fungicides, and identify potential phytocompounds targeting fungal endo-1,3-β-D-glucanase through molecular docking and molecular dynamics simulations. **Materials and Methods:** The pathogen was cultured on different fungal media and incubated under various temperature regimes to determine optimum growth conditions. Antagonistic activity of *Trichoderma harzianum* and *Trichoderma erinaceum*, antifungal activity of selected plant extracts, and the efficacy of commonly used fungicides were evaluated using *in vitro* assays. *In silico* analyses, including molecular docking and molecular dynamics simulations, were performed to assess the binding affinity and stability of selected phytocompounds against fungal endo-1,3-β-D-glucanase. **Results:** Carrot agar and malt agar supported the highest mycelial growth, while the optimum temperature for fungal growth was 25-30°C. *Trichoderma harzianum* exhibited stronger antagonistic activity than *T. erinaceum*. Among the tested phytoextracts, the 30% crude extract of *Lawsonia inermis* produced the greatest inhibition of mycelial growth. Carbendazim and the combination of mancozeb+metalaxyl completely inhibited fungal growth, whereas copper oxychloride showed moderate antifungal activity. Computational analyses identified Diosmetin as the strongest binder to endo-1,3-β-D-glucanase, forming the most stable protein-ligand complex among the evaluated phytocompounds. **Conclusion:** The findings demonstrate that *Lawsonia inermis* extract and *Trichoderma harzianum* are promising eco-friendly alternatives for managing sunflower anthracnose caused by *Lasiodiplodia pseudotheobromae*. In addition, Diosmetin showed strong potential as a natural antifungal inhibitor of endo-1,3-β-D-glucanase, supporting its further investigation through laboratory and field validation studies for the development of sustainable disease management strategies.

KEYWORDS

Anthracnose disease, temperature, endo-1,3-β -D-glucosidase, *L. inermis* phytoextracts, diosmetin

Copyright © 2026 Sikder et al. This is an open-access article distributed under the Creative Commons Attribution License, which permits unrestricted use, distribution and reproduction in any medium, provided the original work is properly cited.

ISSN: 1996-3351 (Print)
https://doi.org/10.3923/ajbs.2026.99.116

Received: 06 Jul. 2026
Accepted: 20 Sep. 2026
Published: 30 Sep. 2026

INTRODUCTION

Sunflower (*Helianthus annuus L.)* is a short-season and fast-growing plant, which grows from summer to autumn, with May usually being the best time to sow sunflower seeds. The perfect temperature for sunflower growth is 20-25°C[1]. Bangladesh is an agricultural country with enormous potential. According to estimates, Bangladesh produced 2006.20, 2728.99, and 3622.11 million tons of sunflower seeds in the fiscal years 2020-21, 2021-22, and 2022-23, respectively[2]. However, fungal diseases are the primary biotic stress in most sunflower cropping systems[3,4]. Among fungal diseases, anthracnose caused by *Lasiodiplodia pseudotheobromae* has recently emerged as a significant threat to sunflower production in Bangladesh, demanding detailed investigation. *Lasiodiplodia* is a genus that belongs to the family Botryosphaeriaceae. Morphologically, both *L. pseudotheobromae* and *L. theobromae* share similar characteristics, and *L. pseudotheobromae* has been considered as the hidden species within the *L. theobromae* complex. Based on conidial features, *L. pseudotheobromae* was separated from *L. theobromae*[5]. *Lasiodiplodia pseudotheobromae* has been found to be associated with post-flowering stalk rot on maize[6], pedicel and peduncle discolouration on grapes[7], necrosis and canker disease on pear tree, and rot and canker on apple, walnut, and hackberry[8].

Although *L. pseudotheobromae* has been reported in sunflower and several other economically important crops, previous studies have mainly focused on disease occurrence and pathogen identification. Detailed information regarding its physiological characteristics, effective biological and chemical management, and molecular characterization of pathogenicity-related proteins remains limited. Furthermore, so far, no study has integrated laboratory experiments with computational approaches to identify potential natural inhibitors against this pathogen. Therefore, a comprehensive investigation combining *in vitro* and *in silico* analyses is needed.

In the search for effective eco-friendly solutions, the screening of bioactive chemicals for their antibacterial and antifungal properties is crucial, as this approach has led to the discovery of structurally distinct bioactive compounds[9]. Computational techniques can screen a greater number of phytocompounds within a short time. Furthermore, this approach can be applied to target protein identification.

Endo-β-1,3-glucanase is involved in fungal cell wall synthesis, hyphal growth, sporulation, host colonization, and degradation of β-1,3-glucan during infection[10]. Since this enzyme contributes to fungal development and pathogenicity, it represents a promising molecular target for identifying environmentally friendly antifungal compounds. Characterizing inhibitors of this enzyme may facilitate the development of alternative disease management strategies with reduced dependence on synthetic fungicides.

Therefore, the present study aimed to characterize the physiological responses of *L. pseudotheobromae* to different fungal culture media and temperature conditions and to assess the efficiency of biological, phytoextracts, and chemical control measures against the fungal pathogen. In addition, molecular docking and molecular dynamics simulations were used to identify effective natural inhibitors of endo-β-1,3-glucanase as candidates for eco-friendly disease management.

MATERIALS AND METHODS

Study area and duration: The present study was conducted in the laboratory of Mycology and Plant Pathology, Department of Botany, Jahangirnagar University, Savar, Dhaka, Bangladesh, during June 2023 to June 2024.

Sample collection: The fungal pathogen was collected from the Culture Collection Center at Jahangirnagar University, Savar, Dhaka, Bangladesh (NCBI accession number: PQ568264). The fungal culture was revived on PDA medium and grew at room temperature (25±2°C) for 7 days. The hyphal tip inoculation method was applied to purify fungal colonies.

***In vitro* physiological study:** The effects of eight individual solid fungal culture media (PDA: Potato dextrose agar, SGA: Sucrose glucose agar, HPA: Honey peptone agar, PSA: Potato sucrose agar, CA: Carrot agar, MA: Malt agar, YEA: Yeast extract agar, HA: Hansen's agar) were also examined to determine the growth response of the pathogen. To determine the optimum temperature for fungal growth, sterilized PDA medium was used in a petri dish and was inoculated with a 2 mm diameter of actively growing fungal disc. The inoculated Petri dishes were incubated at a range of temperature conditions (10, 15, 20, 25, 30, 35, and 40°C). All experiments were conducted using a completely randomized design using six biological replicates. The inoculated Petri dishes were incubated in a controlled growth chamber (25±2°C, 70±5% relative humidity, under a 12 hrs light/12 hrs dark photoperiod). Fungal colony growth was measured after seven days of incubation.

***In vitro* control measures:** In this study, three crude ethanolic phytoextracts (*Lawsonia inermis* L.; *Azadirachta indica* A. Juss.; and *Annona reticulata* L.) were evaluated against the target fungus. Fresh healthy leaves of *Lawsonia inermis*, *Azadirachta indica*, and *Annona reticulata* were collected from healthy plants growing on the Jahangirnagar University campus, Bangladesh. These leaves were washed thoroughly with distilled water, air-dried under laminar airflow, and approximately 10 g of fresh material was crushed with 95% ethanol. The phytoextract was filtered through Whatman No. 1 filter paper and considered as 100% crude extract and stored at 4°C until further use. Requisite quantities of the crude phytoextract were dissolved in ethanol to prepare final desired concentrations of 10, 20, and 30% (v/v).

In addition, two *Trichoderma* species (*Trichoderma harzianum* and *Trichoderma erinaceum*) were used to assess their efficacy against the targeted fungal isolate using dual culture techniques. A 5 mm mycelial disc of *L. pseudotheobromae* and each *Trichoderma* isolate was placed on opposite sides of a PDA plate at an equal distance. Plates were inoculated only with the fungal pathogen used as controls. These cultures were incubated in a controlled growth chamber (25±2°C, 70±5% relative humidity, under a 12 hrs light/12 hrs dark photoperiod) for seven days. Radial growth inhibition was calculated by measuring colony diameter. Six replicate plates were prepared for each treatment.

Moreover, three commercially available fungicides, namely, Kazim 80 WG (carbendazim), Copper blue 50 WG (copper oxychloride), and Mycogourd (Mancozeb+Metalyxil) were evaluated at different concentrations (Copper Blue: 1500, 2000, 2500ppm, Kazim: 500, 1000, 1500ppm, Mycoguard: 1000, 1500, 2000 ppm) against the radial growth of the pathogenic fungus using the food poison technique. Data on radial growth were recorded after 7 days post-incubation (dpi), and the following formula was used to determine the growth inhibition (%):

$$I\frac{(C-T)}{C}\times 100$$

Where:
I: Percentage of growth inhibition
C: Fungal radial growth on control plate
T: Fungal radial growth on treatment plate

Statistical analysis: Experimental data were analyzed using SPSS version 16.0. At first, the data was checked for normality and homogeneity of variance. One-way Analysis of Variance (ANOVA) was executed to determine treatment effect, followed by Duncan's Multiple Range Test (DMRT) at $p<0.05$. Data were presented as mean Values±Standard Error (SE).

***In silico* fungicide prediction against the fungus:** The selection of effective phytocompounds through virtual screening and the development of biogenic compounds against the target pathogen were performed using *in silico* approaches.

Target protein selection: Endo-1,3-beta-D-glucosidase was selected as a target protein from *L. theobromae* because of its functional activity in cell expansion, cell-cell fusion, release of spores during sporulation, and degradation of host β-glucan[11]. The protein structure was retrieved from AlphaFold Structure Database[12]. The predicted structure was refined using GalaxyWeb, and the models were valuated through RMSD, MolProbity, clash score, Ramachandran favored regions, ERRAT value, and VERIFY3D value[13]. The Ramachandran favored, ERRAT, and VERIFY3D values were determined by SAVESv6.1-Structure Validation Server. Additionally, the binding sites of the selected model were predicted by BIOVIA Discovery Studio and CASTp 3.0, and the structure was prepared for molecular docking[14].

Phytocompounds selection: Phytocompounds derived from *L. inermis* were sourced from the NPASS data sources, and their structural information was retrieved from the PubChem database[15]. The drug-like characteristics and ADMET profiles of the phytocompounds were evaluated through the web server SwissADME. Canonical SMILES data for each phytocompound were retrieved from the PubChem database and utilized in these servers. SwissADME applies a series of guidelines, including Lipinski's rule of six, Muegge's, Veber's, Ghose's, and Egan's rules, to evaluate the compounds for fungicide-like properties[16]. Once the screening was complete, the phytocompounds were prepared for molecular docking via the Molecular Graphics Laboratory (MGL) tool.

Molecular docking: The molecular docking aimed to identify optimal binding interactions between the compounds and the targeted protein. AutoDock Vina was employed to perform the docking study by Shawan *et al.*[17]. The protein and ligands were prepared using the MGL tool, with water molecules removed and hydrogen atoms added before being saved in PDBQT format[18]. The grid box for the protein's binding site was defined based on binding pocket data, with the center positioned at fixed coordinates: X = 0.109, Y = -1.888, and Z = -3.744. The grid box dimensions were set to 58.14×60.637×97.554 Å to ensure comprehensive coverage of the binding region. A commercial fungicide, carbendazim, was used as a control drug for comparing the outcomes of the phytocompounds. The poses with the most negative affinity scores were then selected for further stability assessment through molecular dynamics simulations.

Molecular dynamics (MD) simulation: To assess the binding stability of the selected phytocompound and the control with endo-1,3-beta-D-glucosidase, MD simulations were conducted. Desmond, which runs on the Linux operating system, was utilized for this purpose. The hydration of the complexes was achieved through the System Builder tool, applying a cubic three-point transferable interaction potential (TIP3P) model. The generated model was equilibrated to a physiological salt concentration of 0.15 M by introducing Na^+ and Cl^- ions. For optimal energy efficiency, the OPLS3e force field was employed. The MD simulation ran under isothermal-isobaric (NPT) conditions, set to a temperature of 310 K and a pressure of 1.013 bar. The recording interval of the simulation was 100 ps, and trajectories were saved as 1000 frames[19].

RESULTS AND DISCUSSION

Assessment of the effects of culture media on fungal growth: Most fungal culture media supported the mycelial growth of *L. pseudotheobromae*, although significant differences were observed among the evaluated media ($p<0.05$) (Fig. 1). Carrot agar (CA) and malt agar (MA) supported the greatest vegetative growth, followed by potato dextrose agar (PDA) and Hansen's agar (HA), whereas Sabouraud glucose agar (SGA) showed the lowest fungal growth. These findings suggest that nutrient composition strongly influences the vegetative growth of the pathogen. These could be due to a rich supplement of carbohydrates, vitamins, and other nutrients that promote hyphal growth and development. Similar growth responses have been reported for other *Lasiodiplodia* species. For example, PDA, MA, and V8 juice

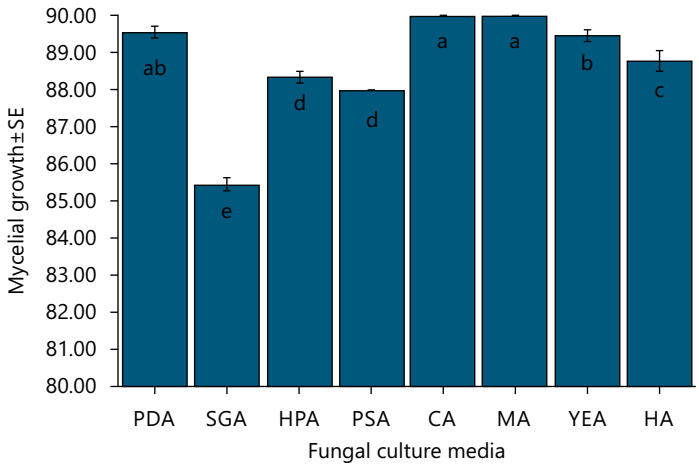


Fig. 1: Effect of culture media on the vegetative growth of *L. pseudotheobromae*

The significant difference is presented as the different letters on the top of bar chart and the same letter does not differ significantly (DMRT), *p<0.05. PDA: Potato dextrose agar, SGA: Sabouraud dextrose agar, HPA: Honey peptone agar, PSA: Potato sucrose agar, CA: Carrot agar, MA: Malt agar, YEA: Yeast extract agar and HA: Hansen's agar

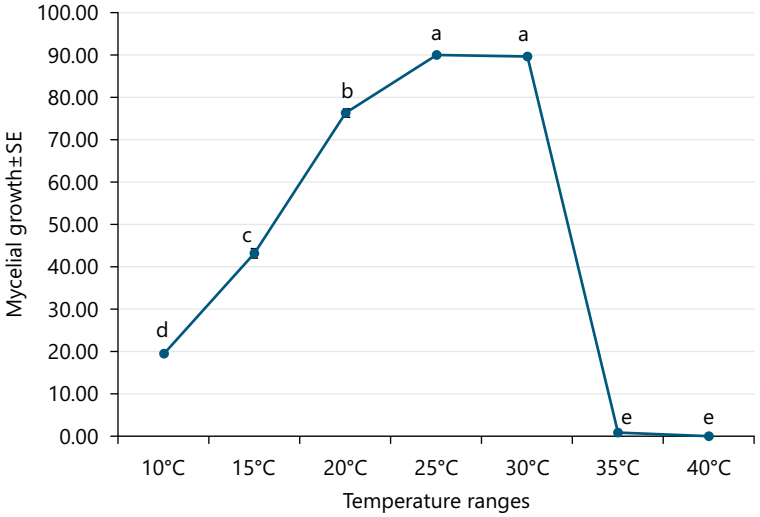


Fig. 2: Effect of temperature on the vegetative growth of *L. pseudotheobromae*

Significant differences are presented as the different letters on the top of data points and the same letter does not differ significantly (DMRT), *p<0.05, and the value represents the Mean±Standard Error (SE) of six replications

gar supported vigorous mycelial growth of *L. theobromae*[20], while PDA and potato stem exudate medium were reported as the most suitable media in another lab bioassay[21]. Likewise, potato sucrose agar promoted substantial vegetative growth in *L. theobromae*[22]. The differences among studies may reflect variations in fungal isolates, origin, and culture medium composition.

Assessment of the effects of temperature on fungal growth: The vegetative growth of *L. pseudotheobromae* was significantly influenced by temperature conditions ($p<0.05$) (Fig. 2). Mycelial growth was found to progressively increase with increasing temperature, reaching an optimum between 25 and 30°C, afterwards, mycelial growth declined abruptly and stopped completely at 35 and 40°C. These findings suggest that *L. pseudotheobromae* is adapted to warm environmental conditions but has a comparatively narrow optimum temperature for vegetative growth. These could be associated with optimal enzymatic activity, nutrient utilization, and cellular metabolism that support vigorous hyphal growth. Notably, higher temperatures may impair enzyme activity, cell membrane stability, and other physiological metabolic processes, which restricted fungal growth.

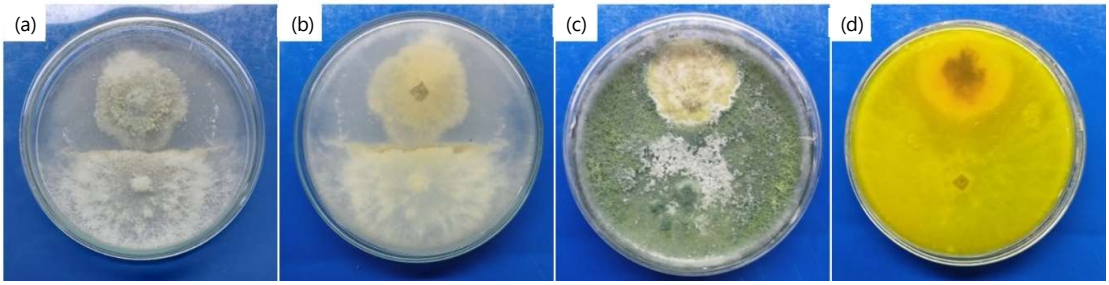


Fig. 3(a-d): Effect of antagonistic fungi on the mycelial growth of the targeted fungus, For each treatment, the left image (a, c) shows the upper view of the fungal colony, whereas the right image (b, d) shows the reverse (lower) view of the same colony
a, b: *Trichoderma erinaceum* vs. *L. pseudotheobromae* and c, d: *Trichoderma harzianum* vs. *L. pseudotheobromae*

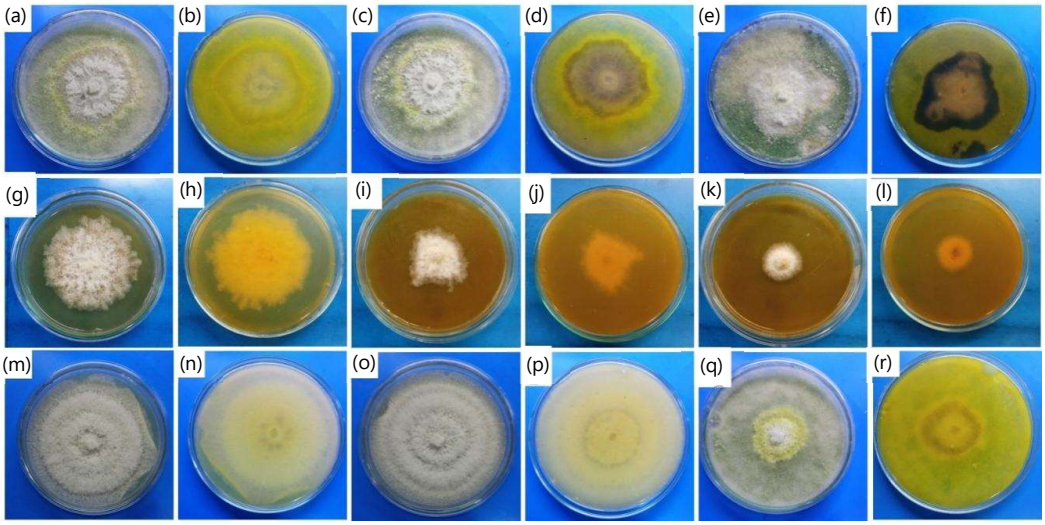


Fig. 4(a-r): Effect of different concentrations of phytoextract-amended PDAmedia on the radial growth of the target fungus, For each treatment, the left image (a, c, e, g, i, k, m, o, q) shows the upper view of the fungal colony, whereas the right image (b, d, f, h, j, l, n, p, r) shows the reverse (lower) view of the same colony. Treatments were: a-b. *Annona reticulata* (10%), c-d: *Annona reticulata* (20%), e-f: *Annona reticulata* (30%), g-h: *Lawsonia inermis* (10%), i-j: *Lawsonia inermis* (20%), k-l: *Lawsonia inermis* (30%), m-n: *Azadirachta indica* (10%), o-p: *Azadirachta indica* (20%), and q-r: *Azadirachta indica* (30%)

Our findings conform with previous studies that reported *Lasiodiplodia* species exhibited optimum growth between approximately 25 and 30°C. For instance, Alam *et al.*[23] cited that 29°C was optimal for mycelial growth, whereas the maximum sporulation found between 25 and 30°C. Likewise, Fovo *et al.*[20] cited that vegetative growth and sporulation of *L. theobromae* increased with temperature up to 28°C, with mycelial growth ceased over 33°C. These findings indicate that warm temperatures are favorable for the development of *Lasiodiplodia* species and may increase the risk of disease incidence under tropical and subtropical environments.

Impact of biocontrol agents and plant extracts: Among the two *Trichoderma* species tested, *Trichoderma harzianum* showed potential antagonistic activity against *L. pseudotheobromae* than *T. erinaceum* (Fig. 3a-d and 5). *T. harzianum* restricted approximately 60% of vegetative growth and completely encircled the fungal colony, whereas *T. erinaceum* showed only moderate inhibition (35%) and did not able to overgrow the pathogen. The direct interaction noticed between *T. harzianum* and *L. pseudotheobromae* suggests that this biocontrol agent possesses antagonistic potential against the targeted pathogen under lab bioassay conditions. The greater inhibitory effect of *T. harzianum* is most

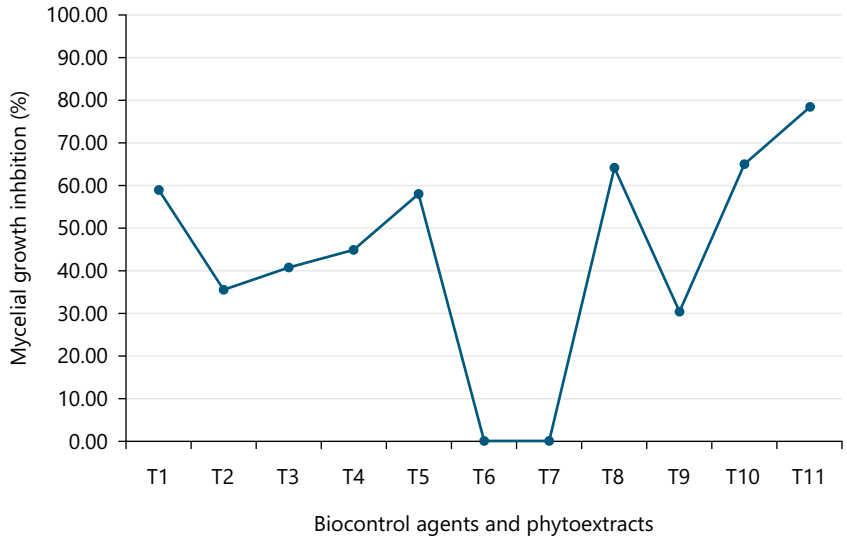


Fig. 5: Effect of biocontrol agents and phytoextracts on the vegetative growth inhibition of *L. pseudotheobromae*

T1: *Trichoderma harzianum*, T2: *Trichoderma erinaceum*, T3: *Annona reticulata* (10%), T4: *Annona reticulata* (20%), T5: *Annona reticulata* (30%), T6: *Lawsonia inermis* (10%), T7: *Lawsonia inermis* (20%), T8: *Lawsonia inermis* (30%). T9: *Azadirachta indica* (10%), T10: *Azadirachta indica* (20%) and T11: *Azadirachta indica* (30%). Mycelial growth inhibition (%) was calculated using six replicates

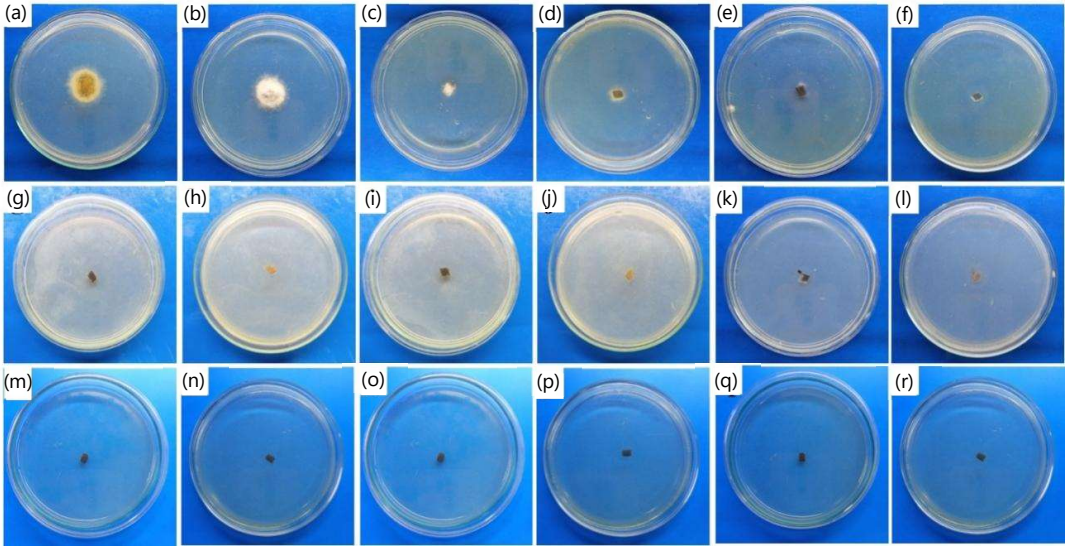


Fig. 6(a-r): Effect of different fungicides incorporated into PDA medium on vegetative growth of the target fungus, For each treatment, the left image (a, c, e, g, i, k, m, o, q) shows the lower view of the fungal colony, whereas the right image (b, d, f, h, j, l, n, p, r) shows the corresponding reverse (upper) view. Treatments were: a-b: Copper Blue (1500 ppm), c-d: Copper Blue (2000 ppm), e-f: Copper Blue (2500 ppm), g-h: Kazim (500 ppm), i-j: Kazim (1000 ppm), k-l: Kazim (1500ppm), m-n: Mycoguard (1000 ppm), o-p: Mycoguard (1500 ppm) and q-r: Mycoguard (2000 ppm)

likely associated with multiple antagonistic mechanisms such as rapid growth, competition for available nutrients and space, mycoparasitism, and the formation of antifungal metabolites and cell wall-degrading enzymes. Our findings are consistent with previous reports indicating the effectiveness of *Trichoderma* species against *Lasiodiplodia* spp. For instance, *Trichoderma* isolates have been shown to suppress the growth of *L. theobromae* via mycoparasitism and antagonistic interactions[24]. Microscopic studies have

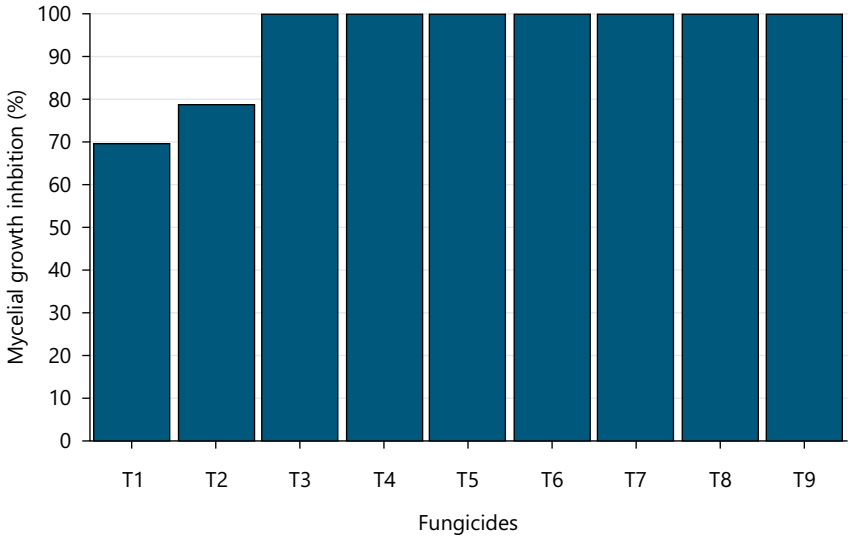


Fig. 7: Effect of fungicides on the vegetative growth inhibition of *L. pseudotheobromae*

Here, T1: Copper blue (1500 ppm), T2: Copper blue (2000 ppm), T3: Copper blue (2500 ppm), T4: carbendazim (500 ppm), T5: carbendazim (1000 ppm), T6: carbendazim (1500 ppm), T7: Mycogourd (1000 ppm), T8: Mycogourd (1500 ppm), T9: Mycogourd (2000 ppm) and Mycelial growth inhibition (%) was calculated using six replicates

revealed hyphal coiling, direct parasitism, and cell wall degradation of *L. theobromae* by *T. harzianum*[25]. The present results suggest that *T. harzianum* could be used as a promising biological control agent for managing sunflower anthracnose.

All three phytoextracts showed an antifungal activity against *L. pseudotheobromae*, although their efficacy varied among treatments (Fig. 4a-r and 5). The mycelial growth inhibition generally increased with increasing phytoextract concentration, with the 30% treatments showing the utmost suppression of fungal growth. Among the evaluated phytoextracts, *Lawsonia inermis* was the most effective, reached 78% mycelial growth inhibition, followed 64 and 58% by *Azadirachta indica* and *Annona reticulata*, respectively. On the contrary, the lower concentrations (10 and 20%) of *A. indica* showed minimal inhibitory effect, indicating a concentration-dependent antifungal efficacy. The potential antifungal activity of *L. inermis* is likely due to its high content of bioactive secondary metabolites, such as flavonoids, phenolic compounds, tannins, quinones, xanthones, gallic acid, and lawsone (2-hydroxynaphthoquinone), which is reported to disintegrate fungal cell membranes and obstruct mycelial growth[26-28]. Likewise, the concentration-dependent inhibition observed for *A. indica* may be associated with the accumulation of antifungal phytochemicals such as glycosides and saponins, which become more effective at higher concentrations[29-31]. Although *A. reticulata* exhibited comparatively lower inhibition, its moderate antifungal activity suggests that it also contains bioactive compounds such as glycosides, saponins, tannins, flavonoids, and phenols capable of suppressing fungal development[32,33].

Impact of fungicides on the targeted fungus: All three fungicides exhibited significant antifungal activity against *L. pseudotheobromae* under *in vitro* conditions (Fig. 6a-r and 7). Among the tested products, Kazim (carbendazim) and Mycogourd (mancozeb + metalaxyl) were the most effective, inhibiting mycelial growth completely at all tested concentrations. In contrast, Copper Blue (copper oxychloride) exhibited a concentration-dependent inhibitory effect, with complete inhibition recorded only at the highest concentration (2500 ppm), whereas lower concentrations showed moderate suppression of fungal growth. These results indicate that carbendazim and the mancozeb+metalaxyl combination fungicide provided the most effective control of *L. pseudotheobromae* compared with copper oxychloride under *in vitro* conditions.

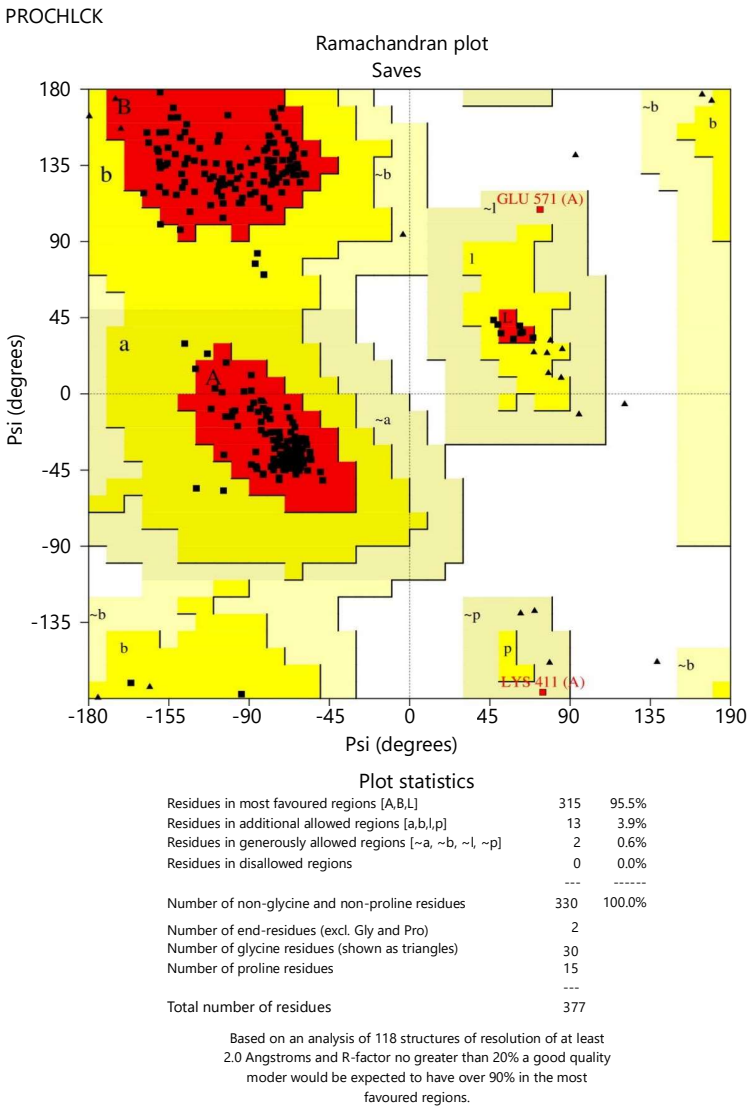


Fig. 8: Ramachandran plot of the selected model

95.5% of residues were located in the favored region; 3.9% of residues remained in additional allowed regions; generously allowed regions consisted of 0.6% residues; No residues in the disallowed regions. 330 amino acids from 377 amino acid residues are situated in the favored region

The high efficacy of carbendazim and the mancozeb+metalaxyl formulation is likely associated with their antifungal modes of action. Carbendazim is known to disrupt microtubule assembly during mitosis, thereby inhibiting fungal cell division, whereas mancozeb acts as a multi-site contact fungicide that interferes with several cellular metabolic processes. In contrast, copper oxychloride usually disrupts fungal enzymes and membrane integrity, and may need a higher concentration to completely inhibit mycelial growth.

Previous studies have reported high efficacy of carbendazim against *Lasiodiplodia* species. For example, carbendazim and carbendazim+mancozeb completely stopped the mycelial growth of *L. theobromae* under lab bioassay conditions[34,35]. Field experiments have further demonstrated that carbendazim effectively reduced disease severity and improved plant health in infected mango trees and pineapple[36,37]. The current study demonstrates that carbendazim and the mancozeb+metalaxyl formulation are highly effective against *L. pseudotheobromae* isolated from sunflower. However, dependence on synthetic fungicides may increase the risk of resistance and environmental contamination. Therefore, a combination of effective fungicides with biological control agents and promising plant-based extracts, such as *Lawsonia inermis*, may provide a more sustainable disease control strategy.

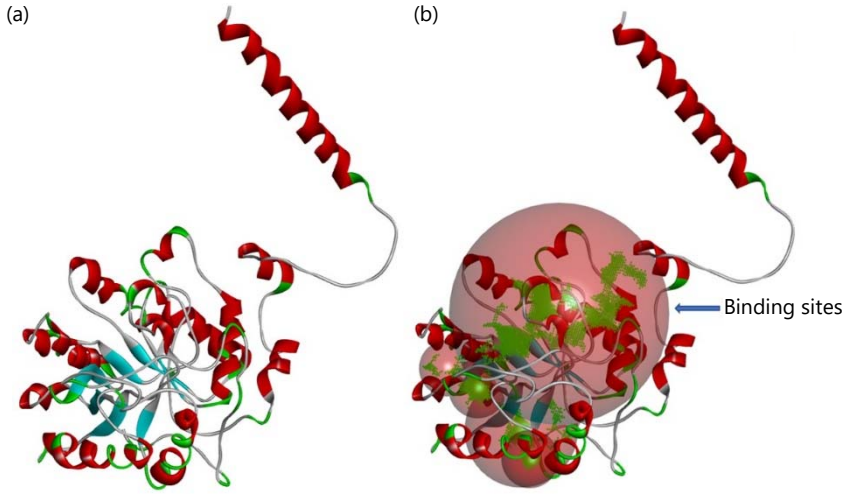


Fig. 9(a-b): Visualization of Glucan endo-1,3-beta-D-glucosidase protein, (a) indicated the 3D structure of the protein and (b) demonstrated the binding sites of the protein

Table 1: Refined models of Glucan endo-1,3-beta-D-glucosidase protein predicted by GalaxyRefine server

Model	RMSD	MolProbity	Clash score	Ramachandran favored region	ERRAT	VERIFY3D
Model 1	0.317	1.437	8.0	95.2	96.01	83.82
Model 2	0.328	1.511	9.7	94.8	96.55	87.00
Model 3	0.298	1.506	8.9	95.5	96.86	88.33
Model 4	0.329	1.504	9.6	94.8	94.87	85.15
Model 5	0.327	1.515	8.2	95.2	95.35	80.64

***In silico* disease management:** The three-dimensional structure of endo-1,3-β-D-glucosidase retrieved from the AlphaFold Structure Database was refined using the GalaxyWeb server. Among the five refined models, Model 3 showed the best overall structural quality based on RMSD, Ramachandran plot, ERRAT, and VERIFY3D analyses (Fig. 8; Table 1). Consequently, Model 3 was selected for subsequent molecular docking because it possessed well-defined ligand-binding pockets (Fig. 9).

A total of 28 phytocompounds from *Lawsonia inermis* were retrieved from the NPASS database. Following pharmacokinetic and fungicide-likeness screening based on the Lipinski, Veber, Ghose, Muegge, and Egan criteria, 12 compounds met the selection criteria and were subsequently used for molecular docking (Table 2 and 3).

The selected phytocompounds were docked against endo-1,3-β-D-glucosidase using carbendazim as the reference fungicide. Ten of the twelve phytocompounds exhibited stronger binding affinity than carbendazim (-5.8 kcal/moL), with Diosmetin showed the utmost binding affinity (-9.1 kcal/moL), followed by Luteolin and Quercetin (Table 4). These findings indicate that several *L. inermis* phytochemicals have strong potential to interact with the target fungal enzyme.

Molecular dynamics simulations were executed to assess the stability of the protein-ligand complexes. All selected complexes remained stable throughout the simulation, as indicated by RMSD, RMSF, hydrogen bonding, and secondary structure analyses (Fig. 10-12). All four protein–ligand complexes formed an initial equilibration phase during approximately the first 10-15 ns, followed by relatively stable RMSD values for the rest of the simulation period (100 ns) (Fig. 10a). Among the four complexes, the Diosmetin-bound proteins exhibited comparatively smaller fluctuations, whereas the Carbendazim complex displayed slightly greater structural deviations throughout the simulation process. Besides, Diosmetin, Quercetin, and Luteolin maintained comparatively consistent RMSD values throughout the simulation (Fig. 10b), which indicates stability within the binding pocket. In contrast, Carbendazim exhibited more pronounced oscillations and intermittent reductions in RMSD, suggesting comparatively

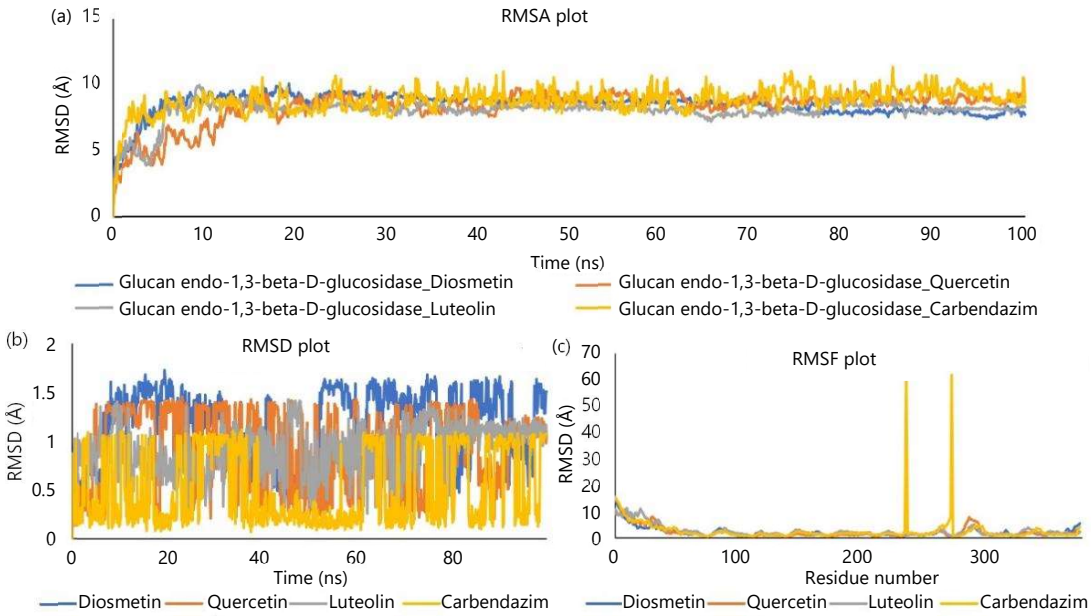


Fig. 10(a-c): Illustration of the graph of the outcomes of the MD simulation. The graph illustrated (a) the RMSD value of the protein backbone regarding the phytocompound and the control (b) RMSD value for the ligands, and (c) RMSF value of the protein residues with the ligands

Table 2: Fungicide likeness properties of the phytocompounds

SL	Phytocompounds	MW (g/moL)	Rotatable bonds	H-bond acceptors	H-bond donors	Lipinski	Ghose	Veber	Egan	Muegge
1	Lupane	412.73	1	0	0	1	3	0	1	2
2	Luteolin-4'glucoside	448.38	4	11	7	2	0	1	1	3
3	Apigenin-4'-Glucoside	432.38	4	10	6	1	0	1	1	2
4	Lawsaritol	414.71	6	1	1	1	3	0	1	2
5	1,3-Dihydroxy-6,7-Dimethoxyxanthone	288.25	2	6	2	0	0	0	0	0
6	Esculetin	178.14	0	4	2	0	1	0	0	1
7	1,4-Naphthoquinone	158.15	0	2	0	0	2	0	0	1
8	Isoquercetin	464.38	4	12	8	2	1	1	1	3
9	Apigetrin	432.38	4	10	6	1	0	1	1	2
10	Astragalin	448.38	4	11	7	2	0	1	1	3
11	Diosmetin	300.26	2	6	3	0	0	0	0	0
12	Isoimperatorin	270.28	3	4	0	0	0	0	0	0
13	Spiraeoside	464.38	4	12	8	2	1	1	1	3
14	Elemicin	208.25	5	3	0	0	0	0	0	0
15	Tilianine	446.4	5	10	5	0	0	1	1	1
16	Daphnorin	514.43	6	12	4	2	1	1	1	2
17	Apiol	222.24	4	4	0	0	0	0	0	0
18	Apiin	564.49	7	14	8	3	3	1	1	3
19	Icariside F2	402.39	7	10	6	1	1	1	1	3
20	Acacetin-7-O-Beta-D-Galactopyranoside	446.4	5	10	5	0	0	1	1	1
21	Kinidilin	300.31	4	5	0	0	0	0	0	0
22	Daphneside	502.42	6	14	8	3	2	1	1	4
23	Quercetin	302.24	1	7	5	0	0	0	0	0
24	Genistein	270.24	1	5	3	0	0	0	0	0
25	2-(3,4-Dihydroxyphenyl)-5,7-Dihydroxy-2,3-Dihydrochromen-4-One	288.25	1	6	4	0	0	0	0	0
26	Phenylethyl Alcohol	122.16	2	1	1	0	3	0	0	2
27	Luteolin	286.24	1	6	4	0	0	0	0	0
28	5-Hydroxy-2-(3-Hydroxy-4-Methoxyphenyl) -7-[(2S,3R,4S,5S,6R)-3, 4,5-Trihydroxy-6-(Hydroxymethyl)Oxan -2-Yl]Oxychromen-4-One	462.4	5	11	6	2	0	1	1	3

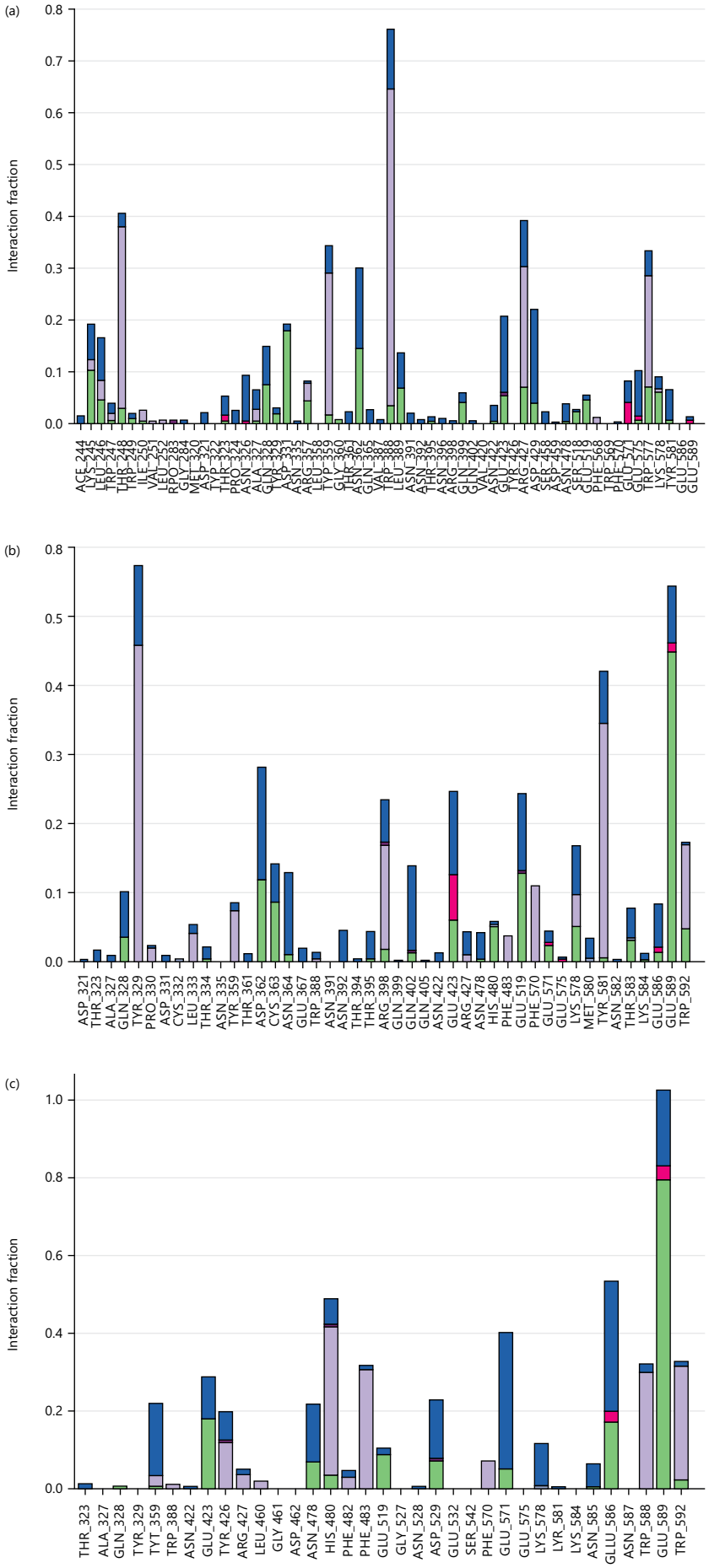


Fig. 11(a-d): Continue

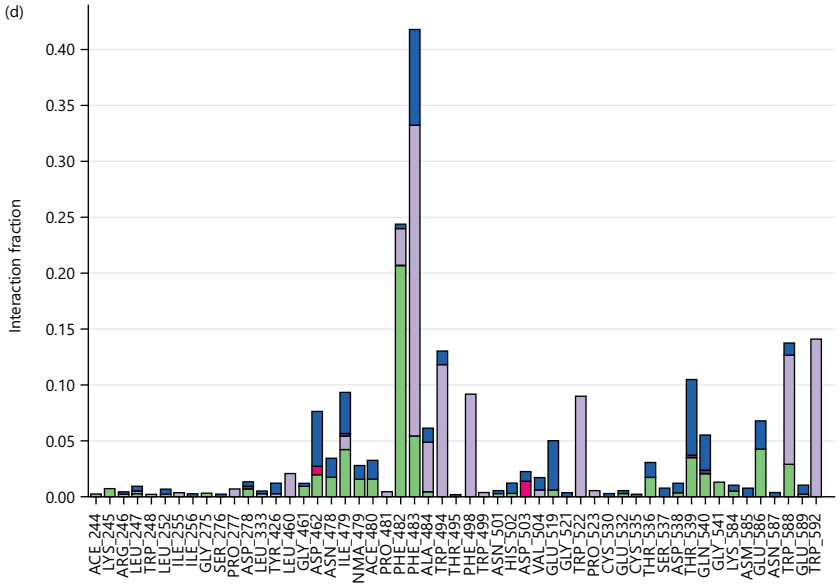


Fig. 11(a-d): Two-dimensional protein–ligand interaction diagrams of the target protein, endo-1,3-β-D-glucosidase, with the selected phytocompounds and commercial fungicide generated from molecular docking analysis, (a) Interaction profile of Diosmetin with endo-1,3-β-D-glucosidase, (b) Interaction profile of Luteolin with endo-1,3-β-D-glucosidase, (c) Interaction profile of Quercetin with endo-1,3-β-D-glucosidase and (d) Interaction profile of Carbendazim with endo-1,3-β-D-glucosidase

The interaction diagrams illustrate hydrogen bonds, hydrophobic interactions, ionic interactions, and water bridges formed between the ligands and amino acid residues within the protein binding site

Table 3: Pharmacokinetics properties of the selected phytocompounds

SL	Phytocompounds	MW (g/moL)	Rotatable bonds	H-bond acceptors	H-bond donors	Lipinski	Ghose	Veber	Egan	Muegge
1	1,3-Dihydroxy-6,7-Dimethoxyxanthone	288.25	2	6	2	0	0	0	0	0
2	Esculetin	178.14	0	4	2	0	1	0	0	1
3	1,4-Naphthaquinone	158.15	0	2	0	0	2	0	0	1
4	Diosmetin	300.26	2	6	3	0	0	0	0	0
5	Isoimperatorin	270.28	3	4	0	0	0	0	0	0
6	Elemicin	208.25	5	3	0	0	0	0	0	0
7	Apiole	222.24	4	4	0	0	0	0	0	0
8	Kinidilin	300.31	4	5	0	0	0	0	0	0
9	Quercetin	302.24	1	7	5	0	0	0	0	0
10	Genistein	270.24	1	5	3	0	0	0	0	0
11	2-(3,4-Dihydroxyphenyl)-5,7-Dihydroxy-2, 3-Dihydrochromen-4-One	288.25	1	6	4	0	0	0	0	0
12	Luteolin	286.24	1	6	4	0	0	0	0	0

Table 4: Docking results of phytocompounds and standard chemicals with the target protein. The table shows the binding affinity score of phytocompounds and control chemicals with sources

SL	Phytocompounds	Affinity score (kcal/moL)
1	Diosmetin	-9.1
2	Luteolin	-8.9
3	Quercetin	-8.8
4	2-(3,4-Dihydroxyphenyl)-5,7-Dihydroxy-2,3-Dihydrochromen-4-One	-8.6
5	Genistein	-7.9
6	1,3-Dihydroxy-6,7-Dimethoxyxanthone	-6.6
7	Kinidilin	-6.6
8	1,4-Naphthaquinone	-6.3
9	Isoimperatorin	-6.3
10	Esculetin	-6.1
11	Apiole	-5.4
12	Elemicin	-5.2
13	Carbendazim	-5.8

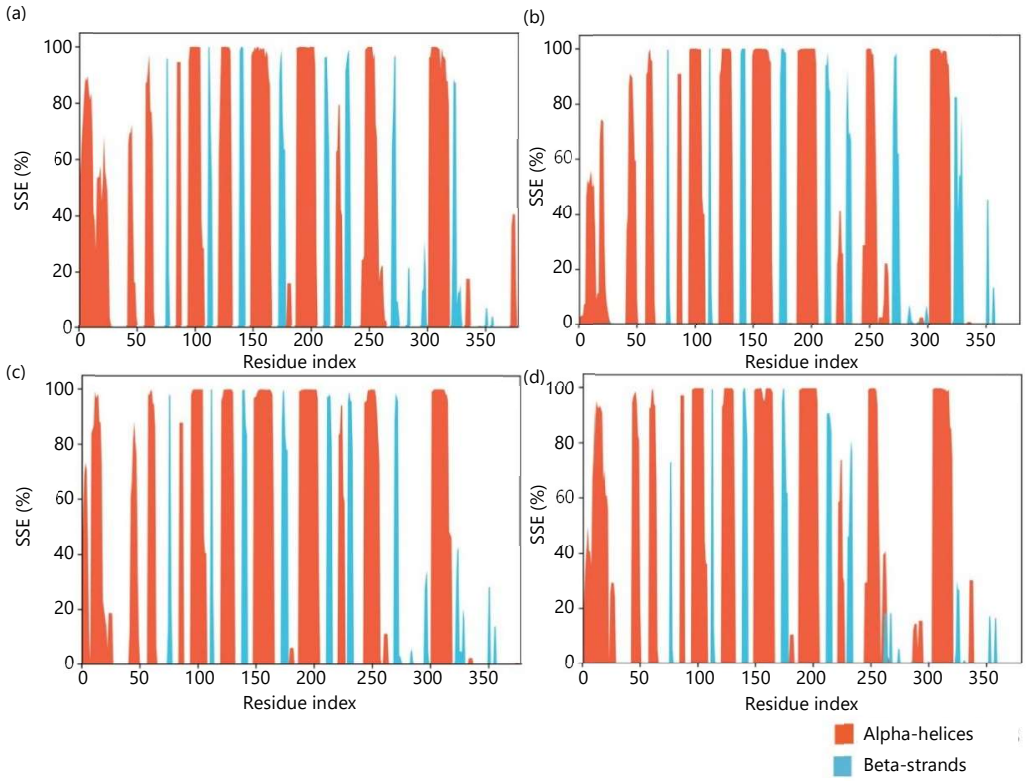


Fig. 12(a-d): Secondary structure element (SSE) analysis of endo-1,3-β-D-glucosidase in complex with the selected phytocompounds and commercial fungicide following molecular dynamics simulation, (a) SSE profile of the endo-1,3-β-D-glucosidase–Diosmetin complex, (b) SSE profile of the endo-1,3-β-D-glucosidase–Luteolin complex, (c) SSE profile of the endo-1,3-β-D-glucosidase–Quercetin complex and (d) SSE profile of the endo-1,3-β-D-glucosidase-Carbendazim complex

The plots illustrate the percentage of secondary structure occupancy across the protein residues, with α-helices shown in orange and β-strands shown in blue

higher mobility and conformational rearrangements during the simulation. The average RMSD values of Diosmetin, Quercetin, Luteolin, and Carbendazim were 1.15, 0.92, 0.92, and 0.52Å, respectively. The values were less than 3 Å, which demonstrated the stability of the complexes during the simulation period[19]. In addition, the residue flexibility analysis (Fig. 10c) further showed that the average RMSF values (less than 3 Å), indicating that the overall protein backbone remained structurally stable irrespective of the bound ligand. Notably, the reference Carbendazim complex displayed two prominent RMSF peaks around residues approximately 240 and 270, reflecting localized increases in residue mobility, which were not observed for the Diosmetin, Quercetin, and Luteolin (Fig. 10c). Overall, among the evaluated compounds, Diosmetin exhibited the lowest protein backbone RMSD (2.28 Å) and RMSF (2.23 Å), indicating a more stable interaction with endo-1,3-β-D-glucosidase than the reference fungicide carbendazim (Fig. 10 a-c). These findings suggest that Diosmetin forms a stable complex with the target protein and therefore represents the most promising phytocompound identified in this study.

The docking analysis showed that Diosmetin formed multiple interactions with residues in the active site of endo-1,3-β-D-glucosidase (Fig. 11a). Luteolin exhibited a distinct interaction pattern involving hydrogen bonds and hydrophobic contacts (Fig. 11b). Quercetin established the highest number of stabilizing interactions with the binding pocket (Fig. 11c). In contrast, the commercial fungicide Carbendazim displayed a different binding interaction profile with the target protein (Fig. 11d).

The secondary structure of the endo-1,3-β-D-glucosidase-Diosmetin complex remained largely stable throughout the simulation, with the α-helices and β-strands exhibiting minimal fluctuations (Fig. 12a). A comparable SSE distribution was observed for the Luteolin complex (Fig. 12b). The Quercetin complex also maintained the overall secondary structural integrity of the protein (Fig. 12c), while the Carbendazim complex displayed a similar pattern of α-helical and β-strand occupancy (Fig. 12d).

In silico approaches have become valuable tools for identifying potential antifungal compounds and prioritizing candidates for experimental validation. Previous studies have successfully employed molecular docking and molecular dynamics simulations to identify bioactive phytochemicals against several plant pathogens, including *Xanthomonas oryzae*[38], *Pseudoperonospora cubensis*[39], and *Candida albicans* through inhibition of β-glucanase enzymes[40,41]. Consistent with these reports, the present study identified several *L. inermis* phytocompounds with strong binding affinity toward endo-1,3-β-D-glucosidase, with Diosmetin showed the most suitable docking score and the greatest structural stability during molecular dynamics simulation.

Importantly, the computational predictions are consistent with the *in vitro* experiments, in which *L. inermis* exhibited the strongest antifungal activity among the tested phytoextracts. This agreement suggests that compounds such as Diosmetin may contribute to the antifungal efficacy of *L. inermis* by interacting with endo-1,3-β-D-glucosidase, an enzyme involved in fungal cell wall remodeling, growth, and pathogenicity. Although the exact mechanism remains to be verified experimentally, inhibition of this enzyme could impair fungal development and reduce pathogenicity.

Nevertheless, molecular docking and molecular dynamics simulations give only computational evidence of protein–ligand interactions. Therefore, although Diosmetin represents the most promising candidate identified in this study, the antifungal activity of this compound should be confirmed via enzyme inhibition assays, purified compound bioassays, greenhouse experiments, and field validation before practical application.

CONCLUSION

Lasiodiplodia pseudotheobromae exhibited vigorous vegetative growth on several culture media, with carrot agar and malt agar supporting the highest mycelial growth, and optimum growth found at 25-30°C. Among the biological control agents, *Trichoderma harzianum* showed greater inhibitory activity than *T. erinaceum*, while the 30% ethanolic extract of *Lawsonia inermis* exhibited the strongest antifungal activity among the tested phytoextracts. Carbendazim and Mancozeb+Metalaxyl completely inhibited mycelial growth under *in vitro* conditions. Molecular docking and molecular dynamics simulations identified Diosmetin as the most promising phytocompound of *L. inermis*, which exhibited the highest binding affinity and stable interaction with endo-β-1,3-glucanase. However, these computational findings are preliminary and require further *in vitro* and *in vivo* validation before Diosmetin can be considered a potential eco-friendly antifungal agent against *L. pseudotheobromae*.

SIGNIFICANCE STATEMENT

Sunflower is one of the important oilseed crops in Bangladesh, however, fungal diseases are responsible for substantial reductions in its yield and quality. Sunflower anthracnose is an emerging disease caused by *Lasiodiplodia pseudotheobromae*, for which effective and eco-friendly management strategies are limited. The present study investigated the growth characteristics of the fungal pathogen under different growth media and temperatures and evaluated the potential of bio-control agents, phytoextracts, and available commercial fungicides for disease management. In addition, *in silico* analyses were employed to identify natural phytocompounds that may inhibit a key fungal enzyme involved in growth and infection. The fungus showed the maximum growth on carrot agar and malt agar at 25-30°C temperature.

Among the bio-control agents, *Trichoderma harzianum* and the phytoextract of *Lawsonia inermis* exhibited the highest antifungal activity, while carbendazim and the combination of mancozeb and metalaxyl completely inhibited fungal mycelial growth under *in vitro* conditions. Computer simulations revealed Diosmetin, a natural phytocompound available in *L. inermis*, as the most promising candidate for the target fungal enzyme. Our findings enable us to understand the biology of this emerging fungal pathogen and provide a nature-based solution that combines biological, phytochemical, chemical, and natural-product-based approaches to manage disease. Further greenhouse and field studies are required to confirm the potency of the identified natural compounds.

FUNDING

This research was funded by University Grants Commission of Bangladesh, grant number Crop Science: 39/2021-2022.

REFERENCES

1. Sghaier, A.H., H. Khaeim, Á. Tarnawa, G.P. Kovács, C. Gyuricza and Z. Kende, 2023. Germination and seedling development responses of sunflower (*Helianthus annuus* L.) seeds to temperature and different levels of water availability. Agriculture, Vol. 13. 10.3390/agriculture13030608.
2. Moller, K., R. Eeswaran, A.P. Nejadhashemi and J.S. Hernandez-Suarez, 2023. Livestock and aquaculture farming in Bangladesh: Current and future challenges and opportunities. Cogent Food Agric., Vol. 9. 10.1080/23311932.2023.2241274.
3. Sikder, M.M., M.S. Ahmmed, P. Akter, F.A. Shetu and B. Akhter *et al*., 2024. First report of *Agroathelia rolfsii* (*Sclerotium rolfsii* Sacc.) causing basal stem rot disease on sunflower in Bangladesh. Asian J. Biol. Sci., 17: 448-461.
4. Sikder, M.M., P. Akter, M.S. Ahmmed, B. Akter, N. Binte Alam, S. Sajuti and M.N. Alam, 2024. Black stem of sunflower: An emerging fungal disease caused by *Fusarium solani* in Bangladesh. Asian J. Biol. Sci., 17: 709-719.
5. He, C., H. Wu, Y. Hu, R. Li and J. Lin *et al*., 2024. Detection and characterization of *Lasiodiplodia pseudotheobromae* associated with stem wilt on *Ficus hirta* (Vahl) and its fungicidal sensitivity. Horticulturae, Vol. 10. 10.3390/horticulturae10101069.
6. Swamy, S.D., S. Mahadevakumar, T. Vasanthkumar, K.N. Amruthesh and H.B. Hemareddy *et al*., 2020. First report of *Lasiodiplodia pseudotheobromae* associated with post flowering stalk rot of maize (*Zea mays*) from India. Plant Dis., Vol. 104. 10.1094/PDIS-11-19-2418-PDN.
7. Dissanayake, A.J., W. Zhang, L. Mei, E. Chukeatirote, J.Y. Yan, X.H. Li and K.D. Hyde, 2015. *Lasiodiplodia pseudotheobromae* causes pedicel and peduncle discolouration of grapes in China. Australas. Plant Dis. Notes, Vol. 10. 10.1007/s13314-015-0170-5.
8. Wang, T., X. Yi, Y. Wu, Y. He, N. Hong, G. Wang and L. Wang, 2024. First report of *Lasiodiplodia pseudotheobromae* causing necrosis and canker disease on pear tree in China. Plant Dis., Vol. 108. 10.1094/PDIS-10-23-2217-PDN.
9. Ogbuagu, O.O., A.O. Mbata, O.D. Balogun, O. Oladapo, O.O. Ojo and M. Muonde, 2025. Novel phytochemicals in traditional medicine: Isolation and pharmacological profiling of bioactive compounds. Int. J. Med. Body Health Res., 3: 63-71.
10. Bai, L., J. Kim, K.H. Son, D.H. Shin, B.H. Ku, D.Y. Kim and H.Y. Park, 2021. Novel anti-fungal D-laminaripentaose-releasing endo-β-1,3-glucanase with a RICIN-like domain from *Cellulosimicrobium funkei* HY-13. Biomolecules, Vol. 11. 10.3390/biom11081080.
11. Edison, L.K., S. Shiburaj and N.S. Pradeep, 2018. Microbial Beta Glucanase in Agriculture. In: Advances in Microbial Biotechnology: Current Trends and Future Prospects, Kumar, P., J.K. Patra and P. Chandra (Eds.), Apple Academic Press, New York, ISBN: 9781351248914, pp: 53-72.
12. Shuvo, M.N., T. Al Arian, M.M. Hossain, S.K. Sil and Salequl Islam *et al*., 2026. Integrated *in silico* and *in vitro* assessment of *Azadirachta indica* leaf extract against multi-drug resistant *Citrobacter koseri* and *Staphylococcus saprophyticus*. Sci. Rep., 10.1038/s41598-026-51906-z.

13. Mazumder, B., A. Ganguli, M.A. Akter, T. Al Arian, M.N. Shuvo, M.M. Mim and M.M. Rahman, 2026. *In silico* identification of damaging CDK4 variants linked to cancer pathogenesis: Functional and structural insights. Egypt. J. Med. Hum. Genet., Vol. 27. 10.1186/s43042-026-00843-7.
14. Halder, S.K., I. Sultana, M.N. Shuvo, A. Shil, M.K. Himel, M. Ashraful Hasan and M.M.A.K. Shawan, 2023. *In silico* identification and analysis of potentially bioactive antiviral phytochemicals against SARS-CoV-2: A molecular docking and dynamics simulation approach. Biomed Res. Int., Vol. 2023. 10.1155/2023/5469258.
15. Shuvo, M.N., T. Al Arian, F. Fuad, M.H. Noman, N. Alam, M.K. Himel and A. Shil, 2026. Computational and immunoinformatics approaches for designing phytocompound-based drugs and a multi-epitope vaccine targeting FemA, a cell wall protein of *Staphylococcus aureus*. PLoS ONE, Vol. 21. 10.1371/journal.pone.0346271.
16. Sikder, M.M., M.S. Ahmmed, B. Akter, Nusrat Binte Alam and M.N. Shuvo *et al*., 2026. Characterization, *in vitro* and *in silico* approach for the management of Nigrospora leaf blight disease of guava in Bangladesh. Am. J. Plant Sci., 17: 251-271.
17. Shawan, M.M.A.K., A.R. Sharma, S.K. Halder, T. Al Arian, M.N. Shuvo, S.R. Sarker and M. Ashraful Hasan, 2023. Advances in computational and bioinformatics tools and databases for designing and developing a multi-epitope-based peptide vaccine. Int. J. Pept. Res. Ther., Vol. 29. 10.1007/s10989-023-10535-0.
18. Mazumder, B., M.N. Shuvo, F. Rahman and M. Mahfuzer Rahman, 2026. Computational screening of plant-derived antimicrobial compounds against alpha-hemolysin of *Staphylococcus aureus*. *In Silico* Res. Biomed., Vol. 2. 10.1016/j.insi.2026.100504.
19. Shuvo, M.N., S.K. Halder, N. Alam, M.K. Himel and A. Shil, 2024. Developing phytocompound-based new drugs against multi-drug-resistant *Staphylococcus aureus*. R. Soc. Open Sci., Vol. 11. 10.1098/rsos.231475.
20. Fovo, J.D., D. Dostaler and L. Bernier, 2017. Influence of culture media and temperature on growth and sporulation of *Lasiodiplodia theobromae*, *Pestalotiopsis microspora* and *Fusarium oxysporum* isolated from *Ricinodendron heudelotii* in Cameroon. Int. J. Curr. Microbiol. Appl. Sci., 6: 3098-3112.
21. Suresh, V., B.V. Sagar, N. Sumalatha and M.R. Prasad, 2017. Effect of culture media and different temperatures on mycelial growth and pycnidial production of *Lasiodiplodia theobromae* casual agent of mango gummosis. J. Mycopathological Res., 54: 531-534.
22. Chukunda, F.A. and U.R. Onyeizu, 2019. Influence of culture media, temperature and light/darkness on the mycelial growth of *Lasiodiplodia theobromae* (Pat.). Greener J. Agric. Sci., 9: 113-118.
23. Alam, M.S., M.F. Begum, M.A. Sarkar, M. Rafiqul Islam and M.S. Alam, 2001. Effect of temperature, light and media on growth, sporulation, formation of pigments and pycnidia of *Botryodiplodia theobromae* pat. Pak. J. Biol. Sci., 4: 1224-1227.
24. Khuong, N.Q., D.B. Nhien, L.T.M. Thu, N.D. Trong and P.C. Hiep *et al*., 2023. Using *Trichoderma asperellum* to antagonize *Lasiodiplodia theobromae* causing stem-end rot disease on pomelo (*Citrus maxima*). J. Fungi, Vol. 9. 10.3390/jof9100981.
25. Bhadra, M., A. Khair, M.A. Hossain and M.M. Sikder, 2015. Efficacy of *Trichoderma* spp. and fungicides against *Lasiodiplodia theobromae*. Bangladesh J. Sci. Ind. Res., 49: 125-130.
26. Han, Y., T. Sun, Y. Tang, M. Yang, W. Gao, L. Wang and C. Sui, 2025. Root rot in medicinal plants: A review of extensive research progress. Front. Plant Sci., Vol. 15. 10.3389/fpls.2024.1504370.
27. Hassan, M., V.K. Fadayomi, I.G. Innocent and M. Suleiman, 2022. Antifungal effect of henna (*Lawsonia inermis*) extract on pathogenic fungi. Microbiol. Res. J. Int., 32: 15-26.
28. Batiha, G.E.S., J.O. Teibo, H.M. Shaheen, B.A. Babalola and T.K.A. Teibo *et al*., 2024. Therapeutic potential of *Lawsonia inermis* Linn: A comprehensive overview. Naunyn-Schmiedeberg's Arch. Pharmacol., 397: 3525-3540.
29. Ezeonu, C.S., C. Imo, D.I. Agwaranze, A. Iruka and A. Joseph, 2018. Antifungal effect of aqueous and ethanolic extracts of neem leaves, stem bark and seeds on fungal rot diseases of yam and cocoyam. Chem. Biol. Technol. Agri., Vol. 5 10.1186/s40538-018-0130-3.

30. Grayer, R.J. and J.B. Harborne, 1994. A survey of antifungal compounds from higher plants, 1982-1993. J. Phytochem., 37: 19-42.
31. Mugford, S.T. and A. Osbourn, 2012. Saponin Synthesis and Function. In: Isoprenoid Synthesis in Plants and Microorganisms: New Concepts and Experimental Approaches, Bach, T.J. and M. Rohmer (Eds.), Springer, New York, United States, ISBN: 978-1-4614-4063-5, pp: 405-424.
32. Simon, K.N., R. Santhoshkumar and N.S. Kumar, 2016. Phytochemical analysis and antimicrobial activities of Annona squamosa (L) leaf extracts. J. Pharmacogn. Phytochem., 5: 128-131.
33. Kalidindi, N., N.V. Thimmaiah, N.V. Jagadeesh, R. Nandeep, S. Swetha and B. Kalidindi, 2015. Antifungal and antioxidant activities of organic and aqueous extracts of *Annona squamosa* Linn. leaves. J. Food Drug Anal., 23: 795-802.
34. Bhure, S.S., P.D. Patil, H.D. Pawar, J.J. Kadam, M.S. Joshi, S.G. Mahadik and S.B. Thorat, 2023. Evaluation of fungicides, phytoextracts and germplasm screening against lasiodiplodia theobromae causing fruit rot of jackfruit. J. Plant Dis. Sci., 18: 26-30.
35. Musdalifa, A.A. and A. Rosmana, 2021. The response of different fungicides against *Lasiodiplodia pseudotheobromae* causing dieback disease of cocoa through *in vitro* test. IOP Conf. Ser.: Earth Environ. Sci., Vol. 807. 10.1088/1755-1315/807/2/022091.
36. Ablormeti, F.K., S.R. Coleman, J.O. Honger, E. Owusu and I. Bedu *et al*., 2021. Management of *Lasiodiplodia theobromae*, the causal agent of mango tree decline disease in Ghana. Afr. Crop Sci. J., 29: 193-207.
37. Oyedeji, E.O. and K.T. Kareem, 2016. *In-vitro* evaluation of some fungicides against *Botrydiplodia theobromae*: Causal pathogen of pineapple dieback. J. Exp. Agric. Int., Vol. 11. 10.9734/AJEA/2016/23238.
38. Joshi, T., S.C. Pandey, P. Maiti, M. Tripathi and A. Paliwal *et al*., 2021. Antimicrobial activity of methanolic extracts of *Vernonia cinerea* against *Xanthomonas oryzae* and identification of their compounds using *in silico* techniques. PLoS ONE, Vol. 16. 10.1371/journal.pone.0252759.
39. Jhansirani, N., V. Devappa, C.G. Sangeetha, S. Sridhara, K.S. Shankarappa and M. Mohanraj, 2023. Identification of potential phytochemical/antimicrobial agents against *Pseudoperonospora cubensis* causing downy mildew in cucumber through *in-silico* docking. Plants, Vol. 12. 10.3390/plants12112202.
40. Shalayel, M.H.F., G.M. Al-Mazaideh, F.K. Al Swailmi, S. Aladaileh, S. Nour, A.T. Afaneh and A. Marashdeh, 2020. Molecular docking evaluation of *Syzygium aromaticum* isolated compounds against exo-β-(1,3)-glucanases of *Candida albicans*. J. Pharm. Res. Int., 32: 34-44.
41. Wadhwa, K., H. Kaur, N. Kapoor and S. Brogi, 2023. Identification of sesamin from *Sesamum indicum* as a potent antifungal agent using an integrated *in silico* and biological screening platform. Molecules, Vol. 28. 10.3390/molecules28124658.